Advances in Materials Physics and Chemistry, 2013, 3, 201-205
http://dx.doi.org/10.4236/ampc.2013.33029 Published Online July 2013 (http://www.scirp.org/journal/ampc)

Controllable Hydrothermal Synthesis of MnO_2 Nanostructures

Jianghong Wu, Hongliang Huang, Li Yu, Junqing Hu*
State Key Laboratory for Modification of Chemical Fibers and Polymer Materials, College of Materials Science and Engineering, Donghua University, Shanghai, China
Email: *hu.junqing@dhu.edu.cn

Received May 2, 2013; revised May 26, 2013; accepted June 4, 2013

ABSTRACT

Various MnO_2 nanostructures with controlling phases and morphologies, like α-MnO_2 nanorods, nanotubes, nanocubes, nanowires and β-MnO_2 cylinder/spindle-like nanosticks have been successfully prepared by hydrothermal method, which is simply tuned by changing the ratio of Mn precursor solution to HCl, $Mn(Ac)_2{\cdot}4H_2O$ or $C_6H_{12}O_6{\cdot}H_2O$, surfactants and reaction temperature and time. The study found out that temperature is a crucial key to get a uniform and surface-smooth nanorod. High ratio of $KMnO_4$ to HCl leads to well dispersed MnO_2 nanorods and changing the precursor of HCl into $Mn(Ac)_2{\cdot}4H_2O$ or $C_6H_{12}O_6{\cdot}H_2O$ results in forming nanowires or nanocubes. Different shapes such as cylinder/spindle-like nanosticks could be obtained by adding surfactants. Since the properties rely on the structure of materials firmly, these MnO_2 products would be potentially used in supercapacitor and other energy storage applications.

Keywords: Hydrothermal; MnO_2; Nanorods; Nanotubes; Nanowires

1. Introduction

Nanostructured manganese dioxides (MnO_2) have been considered as an ideal electrode material for energy storage, such as supercapacitors (also known as electrochemical capacitors (ECs)) [1-4], high-capacity lithium ion batteries [5], lithium-air batteries [6-8] for their advantages of low cost, earth abundance, environmental friendliness and superior performance in energy capacity. So far, numerous efforts have been devoted to synthesize MnO_2 nanostructures and a variety of strategies have been developed, including thermal decomposition, coprecipitation [9], simple reduction [10,11], solid-phase process, hydrothermal method [4], sol-gel [12], microwave process [13], etc. Among these methods, hydrothermal synthesis has attracted more attention because it is easily controlled on the shape of materials, which are simple processed and in large scale. For example, Li *et al.* [14] used hydrothermal route to obtain 3D urchinlike β-MnO_2 constructed of self-assembled nanorods; Qiu *et al.* [15] synthesized MnO_2 nanomaterials by hydrothermal treatment and investigated their catalytic and electrochemical properties. However, the phase and morphology of the MnO_2 nanostructrues are still not well controlled. Since the properties of electrochemical devices extremely rely on the crystalline phase and morphology of MnO_2 nanostructures [16], developing a simple route to synthesize various phases and shape for MnO_2 nanostructures is of fundamental importance. Herein, we demonstrate a one-step hydrothermal route to synthesize MnO_2 nanostructures with well controlling of their phases and morphologies, including α-MnO_2 nanorods, nanotubes, nanocubes, nanowires and β-MnO_2 nanosticks, which are simply tuned by changing the molar ratio of Mn precursor solution to HCl, $Mn(Ac)_2{\cdot}4H_2O$ or $C_6H_{12}O_6{\cdot}H_2O$, surfactants as well reaction temperature and time. We also propose the formation mechanism of MnO_2 nanostructures. These MnO_2 products would be potentially used in supercapasitor applications and other energy storage devices.

2. Experimental Section

2.1. Synthesis

All of the chemical reagents are analytically pure and used as received without further purification. $KMnO_4$, $Mn(Ac)_2{\cdot}4H_2O$, $C_6H_{12}O_6{\cdot}H_2O$ and PVP were purchased from National Chemical Agent. HCl was purchased from Huping Chemistry Industry.

*Corresponding author.

2.1.1. $KMnO_4$ and HCl as the Precursors

In a typical synthesis, 2.5 mmol $KMnO_4$ was dissolved completely in deionized water and then transferred into a 100 mL Teflon-lined stainless steel autoclave, following dropwise adding of 12 mol/L HCl aqueous solution (The molar ratio of $KMnO_4$ to HCl is controlled at 1:8, 1:4 and 1:2). And more deionized water was added to reach 80% fill rate for the autoclave. Hydrothermal treatments were carried out at 180˚C, 160˚C or 140˚C for 24 h, 18 h or 12 h, and then the autoclave was cooled down to room temperature naturally. White precipitates were collected by centrifugation, and washed with deionized water and ethanol several times to remove impurities. Finally, the precipitates were dried in air at 60˚C for 5 h.

2.1.2. $KMnO_4$ and $Mn(Ac)_2{\cdot}4H_2O$ or $C_6H_{12}O_6{\cdot}H_2O$ as the Precursors

A stock solution labeled A was prepared by dissolving 2.5 mmol $KMnO_4$ into deionized water to make a solution with volume of 40 mL. Another stock solution labeled B was prepared by dissolving 5 mmol Mn $(Ac)_2{\cdot}4H_2O$ (or $C_6H_{12}O_6{\cdot}H_2O$) into deionized water to make a solution with volume of 40 mL. Brown precipitate was formed immediately when mix A with B solution. After it becomes a uniform turbid solution by stirring, it was transferred into a 100 mL Teflon-lined stainless steel autoclave, and carried out under hydrothermal treatment at 180˚C or 140˚C for 12 h or 24 h, and then the autoclave was cooled down to room temperature naturally. White precipitates were collected by centrifugation, and washed with deionized water and ethanol several times to remove impurities. Finally, the precipitates were dried in air at 60˚C for 5 h.

2.2. Characterization

The products were characterized by X-ray diffractometer (XRD; Rigaku D/Max-2550 PC) equipped with Cu-Kα Radiation; Scanning electron microscope (JEOL, JSM-5600 LV) equipped with an X-ray energy dispersive spectrometer (EDS) (Oxford, IE 300 X).

3. Results and Discussion

To study the role of the molar ratio of $KMnO_4$ to HCl, we made three different samples with the molar ratio of 1:8, 1:4 and 1:2, respectively. The reaction was carried out at the temperature of 140˚C for 12 h. **Figure 1** shows the morphology of the as-prepared products. As it shows (**Figures 1(a)-(c)**), the products consist of nanorods with the length ranging from 1 to 3 μm. But when we take a closer look at **Figure 1(b)**, as revealed in the picture inserted, these nanorods are hollow in the center with open ends, more like nanotubes. We found that the nanorods synthesized at the molar ratio of 1:8 were aggregated

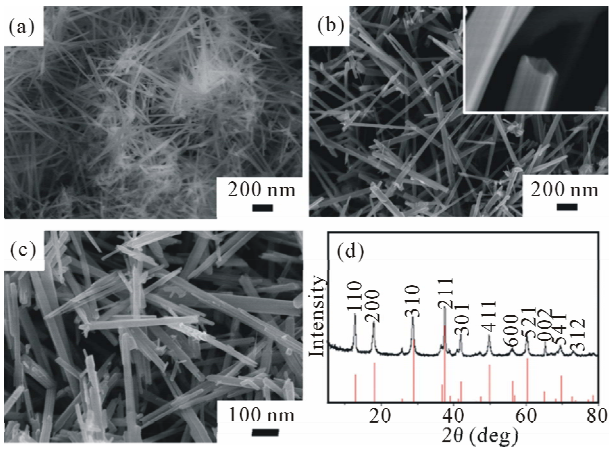

Figure 1. SEM images of the as-synthesized products with the molar ratio of $KMnO_4$ to HCl of (a) 1:8, (b) 1:4 and (c) 1:2. (d) XRD pattern of the as-synthesized products with the molar ratio of $KMnO_4$ to HCl of 1:4. Red line stands for the standard XRD pattern for α-MnO_2.

to some extent with relatively small diameter (30 - 50 nm) and some of these nanorods were entangled to form stab-like spheres with sharp tips, as shown in **Figure 1(a)**. However, this phenomenon was not observed in the ones synthesized at the molar ratio of 1:4 or 1:2, as shown in **Figures 1 (b)** and **(c)**, in which the diameters are wider ranging from 80 to 120 nm. It is likely that a larger amount of HCl (lower ratio of $KMnO_4$ to HCl) leads to the aggragation of nanorods. From the reaction process point of view, the reactions for the formation of MnO_2 use $KMnO_4$ and HCl according to the following reactions: [17].

$$KMnO_4 + H_2O + HCl \rightarrow MnO_2 \cdot H_2O + KCl + H_2O$$

It is obvious that more HCl would accelerate the reaction proceeding to the right, thus more MnO_2 nuclei would be produced within the given time, which is more likely to lead to an aggregation.

The powder X-ray diffraction (XRD; D/max-2550 PC) pattern was shown in **Figure 1(d)** for the sample synthesized with the molar ratio of $KMnO_4$ to HCl of 1:4. The peaks were shown up at the 2θ angle of 12.6˚, 17.9˚, 28.7˚, 36.5˚, 41.8˚, 49.7˚ and 60.2˚. According to the standard value (JCPDS: 44 - 0141), those as-prepared products can be indexed to a tetragonal α-MnO_2 and there is no characteristic peak from impurities. The sharp shape and narrow line widths of the diffraction peaks indicate that the MnO_2 material is highly crystallized. We also performed XRD measurement for another two samples and found out they are in the same crystalline structure.

In order to further explore other parameters that might make impacts on the morphology of the products, we studied the synthesis at different temperatures or time. Moreover, the role of surfactant was also examined. **Figures 2(a)** and **(b)** show the morphology of the as-pre-

pared MnO_2 synthesied at the molar ratio of $KMnO_4$ to HCl of 1:2 at the temperature of 160˚C and 180˚C for 12 h. Similar to the MnO_2 synthesized at 140˚C, the proucts are made of nanorods with length ranging from 1 to 4 μm and diameter from 50 to 200 nm. Compared with the MnO_2 synthesized at 140˚C (**Figure 1(b)**), there are few fine particles on the surfce of MnO_2 nanorods and the higher the temperature is, the fewer the particles on the surface are, which were replaced by a few short nanorods, as shown in **Figure 2(b)**. It is commonly known that nanostructrues start from forming nuclei and then these nuclei would grow up to ressemble into different nanostructures under different conditions. The formation of rods is favored over that of spherical-shaped nanocrystals under the high growth rate regime which usually results from high temperature [18]. This is why we observed that higher temperature leads to short nanorods forming on the surface but not the particles. To study the effect of time, we chose the sample synthsized at 180˚C for 12 h and elongate the reaction time to 18 h. As reveals in **Figure 2(c)**, increasing time doesn't lead to a big variation in the morphology of MnO_2 but the dispersity and uniformity are becoming better with the reaction time increasing. And the surface of the MnO_2 nanorods is more uniform and smoother, and no other impurities on the surface were observed. Additionally, the diameter of these nanorods increases to 50 nm but the length is the same as the ones obtained under lower temperature. **Figure 2(d)** reveals the morphology of the as synthesized MnO_2 by adding PVP as surfactant and the reaction was carried out at the molar ratio of $KMnO_4$ to HCl of 1:2 at 140˚C for 12 h. It is interesting that the MnO_2 nanorods were changed into shorter nanostructures in different shapes, more like cylinder-like and spindle-like nanosticks with the diameter around 1.2 μm. We noticed that the surface of these nanostructures was not as smooth as the one made before but wrinkled.

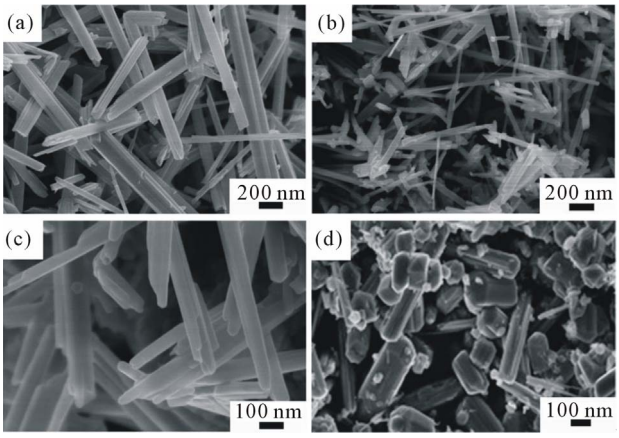

Figure 2. SEM images of the as-synthesized products with the molar ratio of $KMnO_4$ to HCl of 1:2 at (a): 160˚C; (b): 180˚C for 12 h; (c): 180˚C, 18 h; (d): 140˚C, 12 h; PVP was added as surfactant.

XRD was examined to identify the structure for the product obtained by using PVP as surfactant. As **Figure 3** shows, the peaks appear at the 2θ angle of 28.6˚, 37.3˚, 42.7˚, 56.6˚, 59.3˚ and 72.4˚. According to the standard value (JCPDS: 65 - 282), the as-prepared product can be indexed to a tetragonal β-MnO_2 and there are no other characteristic peaks from impurities. The possible reason for the β-MnO_2 formation is proposed as follows: PVP would be absorbed on the surface of MnO_2 nuclei at the beginning of the reaction, resulting in smaller possibility that K+ could take up the 2 × 2 tunnel site in α-MnO_2. Thus, K+ was not able to get into the tunnel to serve as the tunnel stabilizer, finally leading to the formation of small tunnel size β-MnO_2.

Since the molar ratio of $KMnO_4$ to HCl, the temperature and time doesn't change the shape of the MnO_2 nanosturcture significantly, we used $Mn(Ac)_2{\cdot}4H_2O$ and $C_6H_{12}O_6{\cdot}H_2O$ replacing of HCl to explore the effect of precursors on the shape of MnO_2. In order to make a parallel comparison, all reactions were carried out at 180˚C for 24 h. As suggests in **Figures 4(a)** and **(b)**, using HCl results in forming nanorods with length around 3 μm, wich is consistent with the previous results. But when use $Mn(Ac)_2{\cdot}4H_2O$ instead of HCl, long nanowires with the length longer than 5 μm and the diameter of 40 nm were formed, as revealed in **Figures 4(c)** and **(d)**. Interestingly, when $C_6H_{12}O_6{\cdot}H_2O$ was used, the as-prepared samples were formed into hexahedron nanocubes with diameter around 2 μm which are uniform and well dispersed (**Figures 4(e)** and **(f)**).

Figure 5 reveals the XRD pattern of the assynthesized products (**Figures 4(e)** and **(f)**) prepared by using $KMnO_4$ and $C_6H_{12}O_6{\cdot}H_2O$ as the precursors. According to the standard value (JCPDS: 83-1763), the peaks shown in **Figure 5** are consistent with $MnCO_3$ but not MnO_2 which we previously obtained. This is similar to the previous

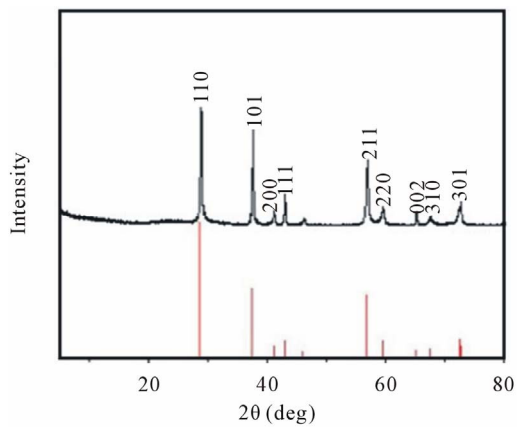

Figure 3. XRD pattern of the as-synthesized products using PVP as surfactant. Red line stands for the standard XRD pattern for β-MnO_2.

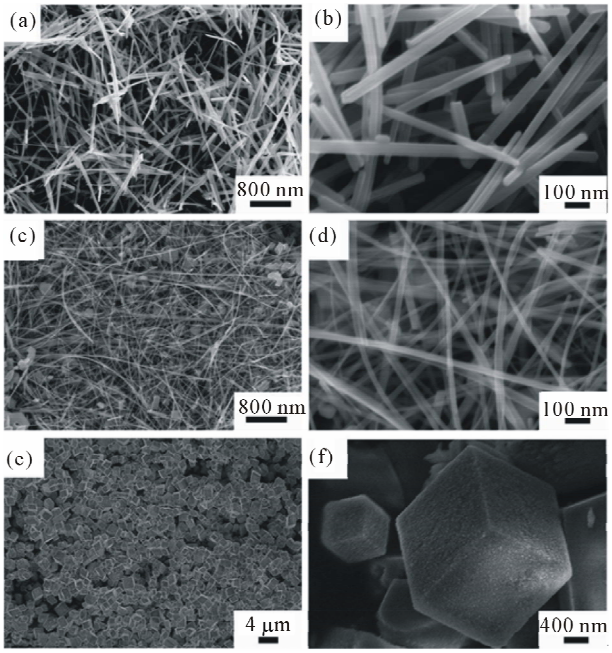

Figure 4. SEM images of the as-synthesized products prepared by using $KMnO_4$ and (a) and (b): HCl; (c) and (d): $Mn(Ac)_2 \cdot 4H_2O$; (e) and (f): $C_6H_{12}O_6 \cdot H_2O$ as the precursors.

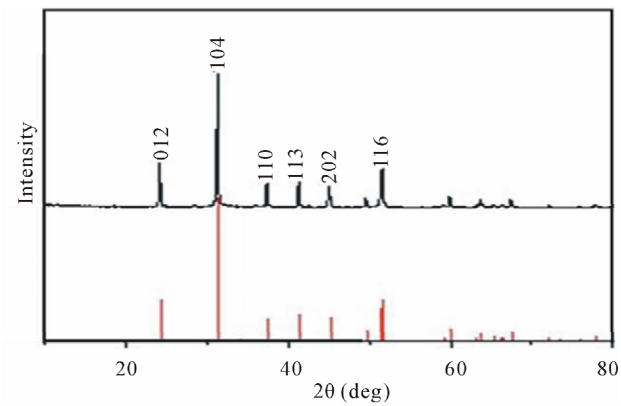

Figure 5. XRD pattern of the as-synthesized products prepared by using $KMnO_4$ and $C_6H_{12}O_6 \cdot H_2O$ as the precursors.

report [19], and MnO_2 could be further obtained by high temperature hydrotreatment according to the literatures [19].

4. Conclusion

In summary, we have synthesized variable MnO_2 nanostructures, including α-MnO_2 nanorods, nanotubes, nanocubes, nanowires and β-MnO_2 cylinder/spindle-like nanosticks which can be achieved by simply tuning the ratio of Mn precursor solution to HCl, $Mn(Ac)_2 \cdot 4H_2O$ or $C_6H_{12}O_6 \cdot H_2O$, surfactants and hydrothermal reaction temperature and time. These morphologies can be simply controlled by only selecting the reactants and controlling experimental conditions with excellent reproducibility. Synthesis process studies of the MnO_2 reveal that temperature is a crucial parameter to get a uniform and surface-smooth nanorod. High ratio of $KMnO_4$ to HCl would lead to well dispersed MnO_2 nanorods. By adding surfactant, different shape such as cylinder/spindle-like nanosticks could be obtained. Changing the precusor of HCl into $Mn(Ac)_2 \cdot 4H_2O$ or $C_6H_{12}O_6 \cdot H_2O$ results in the formation of nanowires or nanocubes. Since the properties rely on the structure of materials firmly, these MnO_2 products would be potentially used in supercapacitor and other energy storage applications.

5. Acknowledgements

This work was financially supported by the National Natural Science Foundation of China (Grant Nos. 21171035, 50872020), the Science and Technology Commission of Shanghai-based "Innovation Action Plan" Project (Grant No. 10JC1400100), Shanghai Rising-Star Program (Grant No. QA1400100), Fundamental Research Funds for the Central Universities, the Shanghai Leading Academic Discipline Project (Grant No. B603), and the Program of Introducing Talents of Discipline to Universities (No. 111-2-04).

REFERENCES

[1] X. Lang, A. Hirata, T. Fujita and M. Chen, "Nanoporous Metal/Oxide Hybrid Electrodes for Electrochemical Supercapacitors," *Nature Nanotechnology*, Vol. 6, No. 4, 2011, pp. 232-236. doi:10.1038/nnano.2011.13

[2] W. Wei, X. Cui, W. Chen and D. G. Ivey, "Manganese Oxide-Based Materials as Electrochemical Supercapacitor Electrodes," *Chemical Society Reviews*, Vol. 40, No. 3, 2011, pp. 1697-1721. doi:10.1039/c0cs00127a

[3] W. Li, G. Li, J. Sun, R. Zou, K. Xu, Y. Sun, Z. Chen, J. Yang and J. Hu, "Hierarchical Heterostructures of MnO_2 Nanosheets or Nanorods Grown on Au-Coated Co_3O_4 Porous Nanowalls for High-Performance Pseudocapacitance," *Nanoscale*, Vol. 5, No. 7, 2013, pp. 2901-2908. doi:10.1039/c3nr34140b

[4] W. Li, Q. Liu, Y. Sun, J. Sun, R. Zou, G. Li, X. Hu, G. Song, G. Ma, J. Yang, Z. Chen and J. Hu, "MnO_2 Ultralong Nanowires with Better Electrical Conductivity and Enhanced Supercapacitor Performances," *Journal of Materials Chemistry*, Vol. 22, No. 30, 2012, pp. 14864-14867. doi:10.1039/c2jm33368f

[5] B. Li, G. Rong, Y. Xie, L. Huang and C. Feng, "Low-Temperature Synthesis of Alpha-MnO_2 Hollow Urchins and Their Application in Rechargeable Li+ Batteries," *Inorganic Chemistry*, Vol. 45, No. 16, 2006, pp. 6404-6410. doi:10.1021/ic0606274

[6] A. Debart, A. J. Paterson, J. Bao and P. G. Bruce, "Alpha-MnO(2) Nanowires: A Catalyst for the O(2) Electrode in Rechargeable Lithium Batteries," *Angewandte Chemie-International Edition*, Vol. 47, No. 24, 2008, pp.

4521-4524. doi:10.1002/anie.200705648

[7] A. K. Thapa, Y. Hidaka, H. Hagiwara, S. Ida and T. Ishihara, "Mesoporous Beta-MnO_2 Air Electrode Modified with Pd for Rechargeability in Lithium-Air Battery," *Journal of the Electrochemical Society*, Vol. 158, No. 12, 2011, pp. A1483-A1489. doi:10.1149/2.090112jes

[8] A. K. Thapa and T. Ishihara, "Mesoporous Alpha-MnO_2/Pd Catalyst Air Electrode for Rechargeable Lithium-Air Battery," *Journal of Power Sources*, Vol. 196, No. 16, 2011, pp. 7016-7020. doi:10.1016/j.jpowsour.2010.09.112

[9] T. Brousse, M. Toupin, R. Dugas, L. Athouel, O. Crosnier and D. Belanger, "Crystalline MnO_2 as Possible Alternatives to Amorphous Compounds in Electrochemical Supercapacitors," *Journal of the Electrochemical Society*, Vol. 153, No. 12, 2006, pp. A2171-A2180. doi:10.1149/1.2352197

[10] P. Ragupathy, D. H. Park, G. Campet, H. N. Vasan, S.-J. Hwang, J.-H. Choy and N. Munichandraiah, "Remarkable Capacity Retention of Nanostructured Manganese Oxide upon Cycling as an Electrode Material for Supercapacitor," *Journal of Physical Chemistry C*, Vol. 113, No. 15, 2009, pp. 6303-6309. doi:10.1021/jp811407q

[11] J. Ni, W. Lu, L. Zhang, B. Yue, X. Shang and Y. Lv, "Low-Temperature Synthesis of Monodisperse 3D Manganese Oxide Nanoflowers and Their Pseudocapacitance Properties," *Journal of Physical Chemistry C*, Vol. 113, No. 1, 2009, pp. 54-60. doi:10.1021/jp806454r

[12] X. Wang, A. Yuan and Y. Wang, "Supercapacitive Behaviors and Their Temperature Dependence of Sol-Gel Synthesized Nanostructured Manganese Dioxide in Lithium Hydroxide Electrolyte," *Journal of Power Sources*, Vol. 172, No. 2, 2007, pp. 1007-1011. doi:10.1016/j.jpowsour.2007.07.066

[13] T. T. Truong, Y. Liu, Y. Ren, L. Trahey and Y. Sun, "Morphological and Crystalline Evolution of Nanostructured MnO_2 and Its Application in Lithium-Air Batteries," *Acs Nano*, Vol. 6, No. 9, 2012, pp. 8067-8077. doi:10.1021/nn302654p

[14] W. N. Li, J. K. Yuan, X. F. Shen, S. Gomez-Mower, L. P. Xu, S. Sithambaram, M. Aindow and S. L. Suib, "Hydrothermal Synthesis of Structure- and Shape-Controlled Manganese Oxide Octahedral Molecular Sieve Nanomaterials," *Advanced Functional Materials*, Vol. 16, No. 9, 2006, pp. 1247-1253. doi:10.1002/adfm.200500504

[15] G. Qiu, H. Huang, S. Dharmarathna, E. Benbow, L. Stafford and S. L. Suib, "Hydrothermal Synthesis of Manganese Oxide Nanomaterials and Their Catalytic and Electrochemical Properties," *Chemistry of Materials*, Vol. 23, No. 17, 2011, pp. 3892-3901. doi:10.1021/cm2011692

[16] S. Devaraj and N. Munichandraiah, "Effect of Crystallographic Structure of MnO_2 on Its Electrochemical Capacitance Properties," *Journal of Physical Chemistry C*, Vol. 112, No. 11, 2008, pp. 4406-4417. doi:10.1021/jp7108785

[17] D. Soundararajan, Y. I. Kim, J.-H. Kim, K. H. Kim and J. M. Ko, "Hydrothermal Synthesis and Electrochemical Characteristics of Crystalline Alpha-MnO_2 Nanotubes," *Science of Advanced Materials*, Vol. 4, No. 8, 2012, pp. 805-812. doi:10.1166/sam.2012.1348

[18] Y. W. Jun, S. M. Lee, N. J. Kang and J. Cheon, "Controll ed Synthesis of Multi-Armed CdS Nanorod Architectures Using Monosurfactant System," *Journal of the American Chemical Society*, Vol. 123, No. 21, 2001, pp. 5150-5151. doi:10.1021/ja0157595

[19] J. Fei, Y. Cui, X. Yan, W. Qi, Y. Yang, K. Wang, Q. He and J. Li, "Controlled Preparation of MnO_2 Hierarchical Hollow Nanostructures and Their Application in Water Treatment," *Advanced Materials*, Vol. 20, No. 3, 2008, pp. 452-454. doi:10.1002/adma.200701231

